Biophysical Journal Volume 98 February 2010 425–433

Recognition and Binding of a Helix-Loop-Helix Peptide to Carbonic Anhydrase Occurs via Partly Folded Intermediate Structures

Martin Lignell and Hans-Christian Becker*
Department of Photochemistry and Molecular Sciences, Uppsala University, Uppsala, Sweden

ABSTRACT We have studied the association of a helix-loop-helix peptide scaffold carrying a benzenesulfonamide ligand to carbonic anhydrase using steady-state and time-resolved fluorescence spectroscopy. The helix-loop-helix peptide, developed for biosensing applications, is labeled with the fluorescent probe dansyl, which serves as a polarity-sensitive reporter of the binding event. Using maximum entropy analysis of the fluorescence lifetime of dansyl at 1:1 stoichiometry reveals three characteristic fluorescence lifetime groups, interpreted as differently interacting peptide/protein structures. We characterize these peptide/protein complexes as mostly bound but unfolded, bound and partly folded, and strongly bound and folded. Furthermore, analysis of the fluorescence anisotropy decay resulted in three different dansyl rotational correlation times, namely 0.18, 1.2, and 23 ns. Using the amplitudes of these times, we can correlate the lifetime groups with the corresponding fluorescence anisotropy component. The 23-ns rotational correlation time, which appears with the same amplitude as a 17-ns fluorescence lifetime, shows that the dansyl fluorophore follows the rotational diffusion of carbonic anhydrase when it is a part of the folded peptide/protein complex. A partly folded and partly hydrated interfacial structure is manifested in an 8-ns dansyl fluorescence lifetime and a 1.2-ns rotational correlation time. This structure, we believe, is similar to a molten-globule-like interfacial structure, which allows segmental movement and has a higher degree of solvent exposure of dansyl. Indirect excitation of dansyl on the helix-loop-helix peptide through Förster energy transfer from one or several tryptophans in the carbonic anhydrase shows that the helix-loop-helix scaffold binds to a tryptophan-rich domain of the carbonic anhydrase. We conclude that binding of the peptide to carbonic anhydrase involves a transition from a disordered to an ordered structure of the helix-loop-helix scaffold.

INTRODUCTION

Molecular recognition of proteins is a fundamental part of many cellular processes (1–4). Several mechanisms have been proposed to explain molecular recognition, for example, the key-lock (5), induced-fit (6), and conformational selection mechanisms (7,8). The key-lock mechanism requires stiff and complementary shapes of the ligands to recognize and bind to each other, whereas the induced-fit mechanism involves a minor conformational change of the receptor induced by the ligand. The conformational selection mechanism, however, assumes a rapid equilibrium of ligand conformations, where the correct and complementary conformation is selected from the ensemble. Several proteins that function as ligands show a transition from a disordered structure in the free form to an ordered structure in the complexed form. These findings suggest that the disordered, unbound structure plays a role in target recognition (9), and that the recognition corresponds to a combined folding and binding process, as proposed in the fly-casting mechanism (10).

Simulation of the thermal unfolding and dissociation of the $p27^{Kip1}$-cyclin A-Cdk2 complex revealed three modes of interaction: a strongly associated complex with a structurally less flexible $p27^{Kip1}$ state, a weakly interacting complex with a flexible $p27^{Kip1}$ state, and a dissociated complex with an intrinsically disordered $p27^{Kip1}$ state (11). The study suggests that recognition and binding of $p27^{Kip1}$ follows a three-step mechanism in which the binding structure of the protein ligand is formed in a hierarchical manner, i.e., the tertiary structure is formed from secondary-structure elements (11). In an experiment by James and Tawfik (12), dynamics between free, intermediate, and bound ligand states were observed by studying the kinetics of binding of fluorescent ligands to an immunoglobin E antibody. The intermediate state was assigned to be an encounter complex that bound the investigated ligands with equal affinity. The formation of the final complex proceeded via an isomerization of the complex with the target-specific ligand. An encounter complex with a nonspecific target ligand was found to dissociate rapidly. Using NMR techniques, small fractions (<10%) of bound protein-protein complexes have also been identified as recognition complexes in which the ligand is less folded (13–17).

The interacting domains of protein structures have characteristic structural fluctuations on several timescales, and for a complete picture, it is often necessary to make measurements using different techniques. NMR measurements of the loop structures that function as complementary determining regions (CDRs) in cameloid heavy-chain antibodies (lacking the light chain) show distinctive structural fluctuations, compared with the non-CDR structures, on the picosecond-to-nanosecond and microsecond-to-millisecond timescales (18). In analogy with the CDR, the loop structures of proline-binding WW domains also show specific fluctuations on the same timescales. The loop structure explores a range of conformations, and a subset of these

Submitted July 14, 2009, and accepted for publication October 1, 2009.
*Correspondence: hcb@fotomol.uu.se
Editor: Alberto Diaspro.

0006-3495/10/02/0425/9 $2.00
doi: 10.1016/j.bpj.2009.10.038

is stabilized when a proline-containing ligand binds to the WW domain. A change of the amino acid sequence of the WW domain alters the intrinsic dynamics and the binding constant of the domain-ligand equilibrium (19). In Namanja et al. (19), the picosecond-to-nanosecond dynamics, as seen by the methyl-specific order parameter, correlated with rotating methyl groups, the motion of which was hindered when the ligand was bound to the flexible WW domain.

Molecular recognition, mediated by a combined folding and binding mechanism, is related to the protein folding problem (20). The folding process is sometimes conceptualized as a reaction on a funneled free-energy landscape (21): folding starts from a large variety of high-energy structures and progresses successively toward the folded state, which is lower in energy and has less conformational diversity. Water may play an important role in this process by guiding the conformational search of the polypeptide to the folded state (22–24), and rate-limiting steps in the folding reaction can lead to the formation of transient structures (25). In this article, we are interested in probing the equilibrium recognition structure(s) that occur between a peptide and a protein using fast time-resolved fluorescence spectroscopy, and in exploring the molecular recognition mechanism between proteins in general.

The peptide used in our experiments (KE2D15-8) was previously developed as a prototype for a peptide-based biosensor (26). It has a helix-loop-helix motif (Ac-NAAD LEAAIRHLAEKLAAR-GPVD-AAQLAEQLAKKFEAFA RAG), and carries on lysine 34 an eight-carbon link with the benzenesulfonamide substrate (Fig. S1 in the Supporting Material), which binds to the active site of the protein human carbonic anhydrase (HCAII). Plain benzenesulfonamide, without the aliphatic spacer and the peptide, binds with a dissociation constant, K_D, of 3000 nM to HCAII. However, the binding strength is increased by three orders of magnitude, to $K_D = 4$ nM, when it is affixed to the helix-loop-helix scaffold (KE2D15-8), which clearly shows the importance of the aliphatic spacer and the helix-loop-helix receptor (26,27). Furthermore, the peptide is modified on lysine 15 with dansyl (Fig. S1), whose fluorescence is sensitive to the polarity of the environment. The binding of the helix-loop-helix peptide to carbonic anhydrase can thus be reported through a change in the photophysical properties of dansyl, as well as through the change in rotational diffusion of the dansyl emission dipole when the dansyl becomes sandwiched between the carbonic anhydrase and the helix-loop-helix surfaces. We use time-resolved fluorescence spectroscopy to resolve fast-fluctuating structures in the peptide-protein interface.

MATERIALS AND METHODS

Lyophilized KE2D15-8 (Fig. S1) and human carbonic anhydrase HCAII (Sigma C-6165, Sigma-Aldrich, Stockholm, Sweden) were reconstituted in 100 mM sodium phosphate buffer (pH 7.20). The peptide is dimeric at high concentration, but dilution experiments (data not shown) show that the dansyl emission shifts significantly to the red upon dilution to the concentration used in the experiments described here (1 μM), indicating that the peptide is monomeric under these conditions. We have no indications that the peptide aggregates into higher-order complexes during reconstitution. Dansylglycine (Sigma D-0875) was used without further purification as the reference fluorophore for measurements of the photophysical properties of dansyl in water, methanol, and ethanol.

Steady-state fluorescence spectroscopy

Binding of the helix-loop-helix peptide to carbonic anhydrase can be detected as a change in the dansyl steady-state emission spectrum. The fluorescence emission spectra between 450 and 650 nm (corrected for wavelength-dependent response) were recorded on a Fluorolog-3 spectrofluorometer (Horiba Jobin-Yvon, Edison, NJ). Titrations were performed by adding KE2D15-8 in steps of 0.1 μM up to 1 μM HCAII. Energy transfer experiments were carried out by exciting the six tryptophans in the carbonic anhydrase enzyme at 290 nm, and detecting the emission from the dansyl on the helix-loop-helix peptide. The apparent energy transfer efficiency was calculated according to Eq. 1:

$$E = 1 - \frac{I_{DA}}{I_D}. \quad (1)$$

Time-resolved fluorescence spectroscopy

Fluorescence lifetime measurements of dansyl and tryptophan were performed using a time-correlated, single-photon counting system described earlier (28). Briefly, pulses (80 fs) of 800 nm light from a Mira oscillator were amplified in a RegA-900 regenerative amplifier connected to an OPA-9000 parametric amplifier, all from Coherent (Santa Clara, CA), generating 670-nm pulses. Vertically polarized 335-nm light for dansyl excitation was subsequently generated by frequency-doubling the 670-nm light using an external BBO crystal. Analogously, for tryptophan excitation, the OPA was adjusted to generate light of 580 nm, which was frequency-doubled to 290 nm.

The instrument response function of the MCP fluorescence detector (Hamamatsu, Hamamatsu City, Japan) was measured using a light-scattering Ludox silica sol sample. Bandpass filters with transmittance at 290 nm and 335 nm (full width at half-maximum $\approx$ 10 nm and 55 nm, respectively) were used in front of the MCP for the tryptophan and dansyl responses, respectively. Fluorescence decays of the tryptophan and the dansyl fluorescence were recorded using magic-angle polarization in the 325–390 nm and 460–600 nm regions, respectively, using different filter combinations. The fluorescence decays were analyzed by iterative reconvolution with the instrument response and a model-free maximum entropy algorithm (29) implemented in MATLAB (The Mathworks, Natick, MA), resulting in a distribution, $P(\tau)$, of fluorescence lifetimes (Eq. 2). The nonbiased initial guess was a vector of time constants, with equal probability, from 0.01 ns to 100 ns, spaced by a factor of $10^{0.01}$ ns. Amplitudes for the different lifetime groups were calculated as the relative area under the peaks of distribution, measured from trough to trough.

$$I(t) = \int_{0.01}^{100} p(\tau)\exp(-t/\tau)d\tau. \quad (2)$$

Time-resolved fluorescence anisotropy

Dansyl fluorescence decays taken with the emission polarized parallel and perpendicular to the vertical polarization of the excitation were recorded. From these recordings, the dansyl anisotropy decays, $r(t)$, were computed using Eq. 3:

$$r(t) = \frac{I_{VV}(t) - I_{VH}G}{I_{VV} + 2I_{VH}G}. \quad (3)$$

The G-factor, which corrects for polarization dependence of the detector sensitivity, was estimated from previous experiments to be 1.0 (Eq. 4):

$$G = \frac{I_{HV}}{I_{HH}}. \quad (4)$$

RESULTS

Steady-state fluorescence of dansyl upon excitation at 335 nm

The fluorescence from dansyl is sensitive to the polarity of the local molecular environment. To characterize the photophysical properties of dansyl in various environments, we measured fluorescence spectra of dansylglycine in water ($\varepsilon_r = 80$), methanol ($\varepsilon_r = 32.7$), and ethanol ($\varepsilon_r = 24.3$) (Fig. S2 *a*). Dansyl emission intensity increases and emission maximum wavelength decreases with decreasing bulk polarity of the solvent. The instrument-response-corrected emission maximum, calculated as the center of gravity of the emission spectrum (30), is 613 nm in water, 573 nm in methanol, and 567 nm in ethanol. In water, the dansylglycine fluorescence is strongly quenched compared to the emission in the moderately polar alcohols. Because of the change in polarity upon binding of carbonic anhydrase to the helix-loop-helix peptide, the complexation can be detected as a change in the dansyl emission.

A continuous increase of the dansyl fluorescence intensity and a continuous blue shift of the dansyl emission maximum was observed when carbonic anhydrase was successively titrated into 1 μM of the helix-loop-helix receptor (KE2D15-8) (Fig. 1 *a*). The dansyl emission maximum decreased from 575 nm for the uncomplexed helix-loop-helix peptide to 566 nm at 1:1 protein/peptide stoichiometry, and the dansyl steady-state intensity increased by ~30% relative to free (uncomplexed) KE2D15-8. The increased dansyl steady-state intensity and the blue-shifted fluorescence spectrum of the KE2D15-8/HCAII complex show that a new molecular environment is formed around the dansyl probe when the helix-loop-helix peptide binds to carbonic anhydrase. Further addition of carbonic anhydrase above 1:1 stoichiometry results in a leveling out of the changes in intensity and emission maximum, indicating a 1:1 complex between peptide and protein. The dissociation constant of KE2D15-8/HCAII was determined by titration of 1 μM KE2D15-8 with HCAII in successive steps of 0.1 μM from 0 μM to 2.0 μM. The fluorescence intensity at 535 nm, corrected for the emission intensity in the absence of HCAII, was found to be proportional to the concentration of the KE2D15-8/HCAII complex. The dissociation constant (K_D) was determined by fitting the dansyl fluorescence intensity at 535 nm to a 1:1 binding model (Eq. 5):

$$K_D = \frac{[\text{HCAII}]_{free}[\text{KE2D15} - 8]_{free}}{[\text{KE2D15} - 8/\text{HCAII}]}. \quad (5)$$

This was done as a control to ensure that the experimental conditions corresponded to those used in previous studies. The fit is not perfect, but the results are in good agreement with those obtained by others (26,27). The KE2D15 peptide, which lacks linker and ligand, does not bind to HCAII, and no changes are observed in the emission from the peptide upon addition of HCAII (26).

Time-resolved fluorescence of dansyl upon excitation at 335 nm

The fluorescence lifetime of dansyl, like the emission maximum and intensity, depends on the polarity of the molecular microenvironment. The fluorescence lifetime of dansylglycine is 2.4 ns in water, 11.4 ns in methanol, and 12.8 ns in ethanol. In these solvents, fluorescence decay can be described either by a single exponential or by a very narrow distribution of lifetimes using the maximum entropy method. It is important to note that this comparison gives a measure of the apparent width given by a homogeneous decay using the maximum entropy method. Fig. S2 *b*

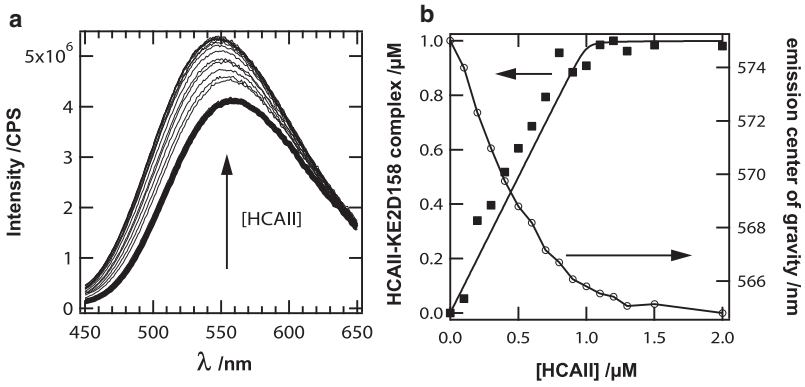

FIGURE 1 (*a*) Dansyl fluorescence spectra of the helix-loop-helix receptor (KE2D15-8). The pure KE2D15-8 spectrum (1 μM) shows the lowest fluorescence intensity and the most red-shifted emission maximum. Addition of carbonic anhydrase (0, 0.2, 0.3, 0.4, 0.5, 0.6, 0.7, 0.8, 0.9, 1.0, 1.1, 1.2, 1.3, 1.5, and 2.0 μM) increases the intensity and blue-shifts the emission maximum. Dansyl fluorescence intensity and changes in emission maximum level out after 1.0 μM. (*b*) Left axis: Concentration of the formed KE2D15-8/HCAII complex when 1 μM of KE2D15-8 is titrated with HCAII up to 2 μM. The concentration of the complex was estimated from the dansyl fluorescence intensity at 550 nm (*solid squares*). K_D was estimated at 1 nM by fitting a 1:1 binding model (Eq. 5) to the concentration of the complex (*solid line*). Right axis: Change of the dansyl emission maximum (*open circles*) as a function of concentration of carbonic anhydrase.

shows the sharp maximum entropy distribution of dansylglycine in these solvents. The lifetime maxima obtained from maximum entropy fitting correspond accurately with those obtained by analysis using a single discrete fluorescence lifetime.

The fluorescence lifetime distribution of dansyl from uncomplexed KE2D15-8 is shown in Fig. 2 (*lower*) (also see Table 1). In contrast to the distribution obtained from dansylglycine, it is extremely broad, suggesting a large variety of helix-loop-helix conformations and corresponding dansyl environments. Since the fluorescence lifetime reflects the polarity of the dansyl microenvironment, we interpret this as a multitude of conformations in which the dansyl is exposed to water to different degrees. Short fluorescence lifetimes indicate hydrated conformations in the dansyl proximity, whereas long fluorescence lifetimes are a sign of dehydrated conformations. In this way, fluorescence lifetime works as a probe of the tertiary structure of the helix-loop-helix peptide. When the helix-loop-helix peptide is bound to carbonic anhydrase, the shape of the dansyl fluorescence lifetime distribution is dramatically different (Fig. 2, *upper*). It becomes divided into three major subdistributions, each of which is much narrower than those of the uncomplexed helix-loop-helix peptide. The appearance of a long fluorescence lifetime group with a peak around 17 ns suggests that dansyl is now part of a new tertiary structure, where it is sandwiched in a hydrophobic environment between carbonic anhydrase and the helix-loop-helix peptide. There are two other fluorescence lifetime groups whose maxima occur at ~8 ns and ~3 ns. We assign these two groups of shorter fluorescence lifetimes to two other types of interacting structures in which the carbonic anhydrase and the helix-loop-helix receptor are less tightly bound (see Discussion).

Fluorescence anisotropy of dansyl upon excitation at 335 nm

Fluorescence anisotropy was measured on free KE2D15-8 and KE2D15-8 complexed with HCAII. For the uncomplexed peptide, two rotational correlation times, 0.21 ns and 2.1 ns, are necessary to describe the decay of the dansyl fluorescence anisotropy (see Table 2 and Fig. S4 *a*). From femtosecond transient absorption and picosecond time-correlated single-photon counting measurements, the rotational correlation time of dansylglycine was estimated as ~60 ps (data not shown). Although the peptide has a high helical content in solution, it is not well structured and has a high degree of molten-globule character (31,32). At the concentrations used in our experiments, the peptide is likely partly dimerized and partly monomeric (27), and the biphasic anisotropy decay can be either a result of two rotational modes in the peptide, or simply a manifestation of the monomer-dimer equilibrium. However, in the peptide/protein complex this is not an issue, as the peptide binds exclusively as a monomer (33).

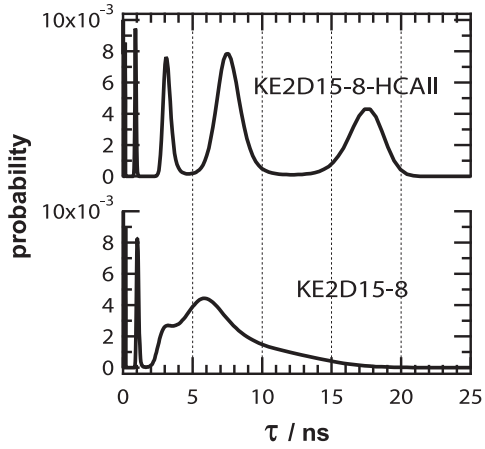

FIGURE 2 Fluorescence lifetime distributions of dansyl from KE2D15-8 complexed 1:1 with carbonic anhydrase (*upper*) and uncomplexed KE2D15-8 (*lower*).

When KE2D15-8 is complexed with carbonic anhydrase, a new rotational correlation time appears (Table 2 and Fig. S4 *b*). Although this new time is shorter than expected for a rigid spherical body of the dimensions of HCAII (40 Å in diameter), it seems likely that it follows the rotational diffusion of the carbonic anhydrase. HCAII is partly unstructured, and other studies have found similar rotational correlation times for proteins of roughly the same size (34). Thus, the emergence of a long rotational correlation time shows that at least a portion of the helix-loop-helix receptor interacts strongly with the surface of carbonic anhydrase.

We have analyzed the anisotropy decay of the KE2D15-8/HCAII complex in two different ways. First, we let all parameters in a three-exponential decay vary freely. This resulted in a 0.18-ns component (22%), a 1.2-ns component (44%), and a 19-ns component (37%). The goodness of fit (χ^2) for this model was 1.09. As this analysis of the fluorescence depolarization gives the same three-component picture as observed in the lifetime distribution (Fig. 2, *upper*), with similar weights for the components, we have tried to connect the anisotropy to the lifetimes using the following reasoning. The short lifetimes (3.1 ns, close to

TABLE 1 Peak maximum fluorescence lifetimes of dansyl for the different maximum entropy subdistributions for free and complexed helix-loop-helix

Dansyl fluorescence lifetimes	Uncomplexed KE2D15-8	Complexed KE2D158:CA
τ_{max1}/ns	0.2 (0.6%)	0.2 (0.5%)
τ_{max2}/ns	1.1 (5.2%)	0.9 (3.1%)
τ_{max3}/ns	3.3 (9.5%)	3.1 (14.4%)
τ_{max4}/ns	5.9 (64%)	7.6 (46%)
τ_{max5}/ns	n/a	17.4 (37%)

Dansyl was excited at 335 nm. Subdistributions are taken from the maximum entropy distributions in Fig. 2. The fraction of each subdistribution, as compared with the total fluorescence lifetime distributions, is given in parentheses. Uncertainties in the data are $< \pm 5\%$.

TABLE 2 Dansyl anisotropy decays for uncomplexed KE2D15-8 peptide, and KE2D15-8 complexed with HCAII at a 1:2 stoichiometric ratio

Anisotropy of dansyl	ϕ_1/ns	ϕ_2/ns	ϕ_3/ns	r_0	χ^2
KE2D15-8	0.21 ± 0.04 (41 ± 7%)	2.1 ± 0.1 (59 ± 2%)	n/a	0.30	1.16
KE2D15-8/HCAII	0.18 ± 0.1 (14 ± 6%)	1.2 ± 0.2 (47 ± 4%)	23 ± 2 (39 ± 2%)	0.27	1.08

Rotational correlation times are given with error margins and the amplitude, which is the fraction r_i compared with r_0. The goodness of fit is given by χ^2.

the 2.4 ns of dansylglycine in water) come from dansyls that are exposed to water. A water-exposed dansyl cannot be buried in the peptide-protein interface or between the helices in a helix-loop-helix structure, and these fluorophores likely have short rotational correlation times. It is important to note that under the experimental conditions used here, there is a negligible amount of free peptide, and we attribute the short-lived fluorescence and short rotational correlation time to peptides that are bound through the ligand and linker to the protein, but not directly to the surface of the protein. In a similar way, fluorophores with long lifetimes are shielded from water by being embedded in hydrophobic domains, and are thus likely to have long rotational correlation times. We have tried to correlate fluorescence lifetime with rotational correlation time by locking the first rotational correlation time (0.18 ns in the first analysis) at an amplitude equal to that of the population (14%) of the 3.1-ns fluorescence lifetime group. The analysis resulted in a slightly modified anisotropy decay model ($\chi^2 = 1.08$): 0.18 ns (14%), 1.2 ns (47%), and 23 ns (39%) (Table 2). It should be noted that using this model, there is almost perfect agreement between the amplitudes of the rotational correlation times and the populations of fluorescence lifetime groups.

Energy transfer from carbonic anhydrase tryptophans to dansyl on the peptide

Irradiation of the KE2D15-8/HCAII complex at 290 nm primarily results in excitation of the tryptophans in HCAII. Compared to the Trp emission of HCAII alone, addition of the dansyl-labeled peptide leads to a decrease in Trp emission intensity (Fig. 3 *a*). The emission from dansyl increases simultaneously, but the increase levels off at 1:1 protein/peptide stoichiometry (Fig. 3 *a*, *inset*). As the emission from tryptophan overlaps significantly with the absorption of dansyl (Fig. 3 *b*), which itself has little absorption at 290 nm, the only plausible mechanism for the increase in dansyl emission upon addition of HCAII is energy transfer from tryptophan to dansyl. At 1:1 stoichiometry of HCAII and KE2D15-8, the tryptophan emission at 333 nm was reduced to ~70% of the unquenched intensity, which resulted in an apparent energy transfer efficiency of 34% (Eq. 1).

Fluorescence lifetime measurements of tryptophan in free and complexed HCAII

Maximum entropy analyses of the tryptophan fluorescence lifetime in free carbonic anhydrase and that in carbonic anhydrase complexed with KE2D15-8 are shown in Fig. S3. For both cases, we observe five subdistributions of tryptophan fluorescence lifetimes. The maximum probable tryptophan lifetimes and the fraction of each subdistribution are summarized in Table S1. The contribution of each fluorescence lifetime to the steady-state intensity was calculated according to Eq. 6:

$$I_{SS} \propto \int p(\tau)\tau d\tau, \tag{6}$$

and from this, an apparent energy transfer efficiency of 37% was calculated (Eq. 1), which is in agreement with the efficiency estimated from the steady-state intensity (see above).

Measurement of the dansyl fluorescence lifetime when excited via tryptophan

Excitation of dansyl in the KE2D15-8/HCAII complex through energy transfer from Trp results in a different dansyl fluorescence decay compared to that obtained by direct

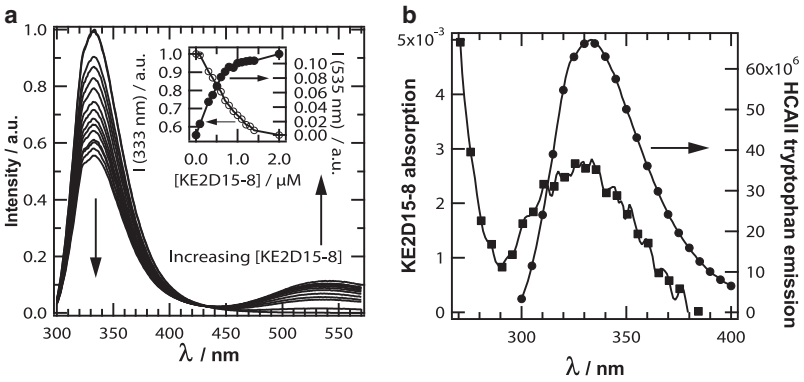

FIGURE 3 (*a*) Emission spectrum of tryptophan (300–400 nm) and of dansyl (440–570 nm) upon excitation at 290 nm of 1 μM HCAII at increasing concentrations of KE2D15-8 (0, 0.1, 0.3, 0.4, 0.5, 0.6, 0.7, 0.8, 0.9, 1.0, 1.1, 1.2, 1.3, 1.4, and 2.0 μM). (*Inset*) Tryptophan and dansyl emission intensities as a function of HCAII concentration. Note the much more rapid increase in dansyl emission during the binding phase (0–1 μM). (*b*) Overlapping absorption spectrum of 1μM KE2D15-8 (*circles*) and emission spectrum of 1μM HCAII (*squares*), mediating Förster energy transfer from tryptophan(s) in HCAII to dansyl on the helix-loop-helix.

excitation at 335 nm. Analysis using discrete lifetimes shows that the sensitized fluorescence contains three components: one in-growing component of 140 ps (−12%), and two decaying components of 8.2 ns (54%) and 18.5 ns (32%) ($\chi^2 = 1.09$). These data were not analyzed using the maximum entropy distribution, since our software does not accurately handle negative amplitudes. If we start the analysis at 330 ps, after the growing-in phase, we can analyze the remaining fluorescence decay using the maximum entropy method. This results in two sharp subdistributions with peak maxima at 8.3 ns (52%) and 18.2 ns (48%) (Fig. 4 *a*). The narrow width of the distributions warrants an analysis of the data using discrete lifetimes, as described below.

Further supporting the energy transfer hypothesis, we found that the 140-ps time constant is also present in the tryptophan decay as a decaying component, but only in the presence of peptide. The $(140\ \text{ps})^{-1}$ rate constant is thus clearly energy transfer from one or more tryptophans in the HCAII to dansyl on KE2D15-8. Based on the estimated Förster energy transfer rate constant, an apparent tryptophan-dansyl distance of 12 Å (Eq. 7) is obtained using $R_0 = 21.5$ Å for the tryptophan-dansyl pair and $\tau_D = 4.1$ ns (35):

$$k_{EET} = \frac{1}{\tau_D} \times \frac{R_0^6}{r^6}. \quad (7)$$

We cannot distinguish which tryptophan is the donor, and the calculated distance merely indicates that the dansyl acceptor is close to one or more tryptophans in the protein (see below).

DISCUSSION

Three interaction structures of KE2D15-8/HCAII

The study of molecular recognition between the helix-loop-helix scaffold and the carbonic anhydrase using time-resolved fluorescence spectroscopy provides details of how recognition is mediated. Analysis of the dansyl fluorescence decay of the KE2D15-8/HCAII complex reveals three major structurally different fluorescence lifetime groups that are formed upon binding of the peptide to the protein. We will focus on the three longest of these groups, which comprise the overwhelming majority (>96%) of the emission. These three dansyl fluorescence lifetime groups (τ_{max3}, τ_{max4}, and τ_{max5} in Table 1) originate in different micropolarities in the different KE2D15-8/HCAII interaction structures. Upon formation of the peptide/protein complex, the fluorescence lifetime distribution goes from broad and featureless to having three distinct peaks (Fig. 2). This change suggests that the peptide is less heterogeneous in each of its bound forms than when it is free in solution, and that the association with the protein helps stabilize three different, characteristic binding structures.

The hydrophobic parts of the protein structure generally have a low dielectric constant (36,37), whereas hydration increases the effective dielectric constant of the hydrated part (38). Dansyl has previously been used to probe the local polarity of polypeptide structures (39), which is why we interpret the peak fluorescence lifetimes as different binding structures in which the peptide is folded to different degrees.

Even though the emission experiments were carried out under conditions such that the concentration of free KE2D15-8 is negligible, we observe a significant fraction of short-lived dansyl emission. This subdistribution, centered around 3.1 ns, has a peak lifetime close to that of dansylglycine in water (2.4 ns; Fig. S2). Hence, we assign to this group, which constitutes 14% of the total complexes, an almost fully hydrated peptide/protein interface. In these structures, the dansyl-carrying part of the peptide makes little contact with the protein despite the fact that the benzenesulfonamide ligand is bound. The dansyl fluorescence lifetime group centered at ~8 ns (46%), however, must stem from less hydrated structures, and thus, likely, a more developed peptide-protein recognition structure. Using the same reasoning, the types of complex giving rise to the fluorescence lifetime group at ~17 ns (37%) correspond to a well-defined and dehydrated structure at the peptide/protein interface. Finally, a small fraction (<4%) of the dansyl emission has a lifetime of <2.4 ns. We have observed this previously (30) and suggest that it is caused by something other than polarity, such as quenching by nearby amino acid residues.

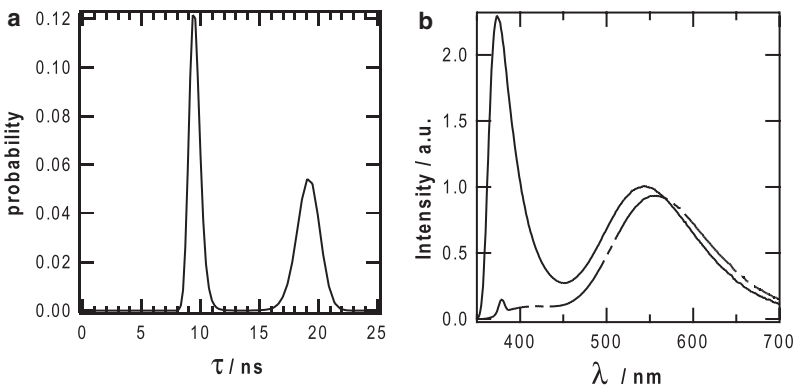

FIGURE 4 (*a*) Dansyl fluorescence lifetime distributions of the KE2D15-8:HCAII complex when dansyl is excited through energy transfer from tryptophan(s) in the HCAII protein. The distribution lacks the 3.1-ns peak, found only when dansyl in the complex is excited directly at 335 nm (compare with Fig. 2). (*b*) Excitation of dansyl in the KE2D15-8/HCAII complex via energy transfer from tryptophans in HCAII results in a blue-shifted dansyl emission spectrum (*solid line*) relative to the directly excited dansyl spectrum at 335 nm (*dashed line*).

The presence of three different binding structures is also reflected in the different rotational correlation times necessary to describe the fluorescence anisotropy decay of the KE2D15-8/HCAII complex (Table 2). We now discuss the results obtained by locking the amplitude of the shortest rotational correlation time to that of the ~3-ns component in the lifetime analysis (see Results). The 23-ns rotational correlation time component, which we believe is associated with the 17-ns fluorescence lifetime component, constitutes 39% of the complexes (Table 2). Such a rotational correlation time is typical for the slow rotational diffusion of a large globular protein like carbonic anhydrase (34). Since our focus of observation is the dansyl, which is linked to the KE2D15-8 peptide, fluorescence lifetime and rotational correlation time data suggest that the fluorophore is protected from water by the protein and the scaffold, and is also rigidly bound to the protein surface. The benzenesulfonamide ligand and the dansyl are on different helices in the peptide, and the fluorescence data thus suggest that both helices must be bound to the protein. NMR indicates strong perturbation of the HCAII surface around the active site (26), and we believe that the dansyls with the long fluorescence lifetime are part of conformations in which dansyl is sandwiched between the surfaces of the helix-loop-helix scaffold and the carbonic anhydrase.

Although amplitude was allowed to vary freely in the analysis, that of the 23-ns anisotropy component, 39%, corresponds well with the fraction of the longest (17 ns) dansyl fluorescence lifetime group, 37%. In all, this strongly suggests that this binding structure of KE2D15-8 to HCAII is characterized by a dehydrated, well-defined tertiary structure that does not allow fast segmental motions of dansyl.

The 1.2-ns rotational correlation time component, however, should come from dansyls that are in a molecular environment where their motion is less hindered. The fraction of dansyl molecules with this rotational correlation time, 47%, corresponds well with the fraction of dansyl fluorophores in the 8-ns fluorescence lifetime group, 46%. This combination of shorter fluorescence lifetime and less hindered rotation is entirely consistent with a more hydrated, more loosely aggregated interface allowing for more rapid motion of the dansyl and more exposure to water. Accordingly, we assign ~50% of the KE2D15-8/HCAII complexes to a partially folded interfacial structural group. This structure, we believe, is equivalent to a molten-globule-like structure with a developed secondary structure of the binding polypeptides, but with a partly hydrated and only partly developed tertiary structure at the interface of the interacting polypeptides (40,41).

The fastest rotational correlation time of dansyl in the complex, 0.18 ns (14%), indicates a molecular environment in which the motion of the fluorophore is quite unhindered. Using the same approach as above, we can correlate the fast fluorescence depolarization with the fraction of almost fully hydrated dansyls with the 3-ns lifetime peak. This is in full agreement with the presence of complexes in which the only principal interaction between peptide and protein is through the substrate and its link.

In molecular dynamics simulations, solvent-separated hydrophobic interactions have been observed in a nativelike compact intermediate, which subsequently forms the native dehydrated form by expelling the water from the solvent-separated states and forming dehydrated hydrophobic interactions (42,43). Accordingly, we think that the formation of the tightly bound peptide/protein structure is assisted at some point by solvent-separated hydrophobic interactions between protein and peptide. We thus believe that the three bound forms we observe are connected to the desolvation of the binding surfaces in at least two sequential steps, and to a disordered-to-ordered transition of the polypeptide upon binding.

Where does the helix-loop-helix peptide bind to carbonic anhydrase?

The crystal structure of carbonic anhydrase (HCAII) (44) shows a nonstructured N-terminus containing five tryptophan residues, and a single tryptophan on the opposite side of the N-terminus surface of HCAII. The N-terminus region is close to the active site and the active-site cleft, where the benzenesulfonamide on the aliphatic linker (C8) goes in. In Fig. 6 of Andersson et al. (26), the helix-loop-helix scaffold is shown to bind to this less structured surface on carbonic anhydrase, which was confirmed by NMR (26). We can use Förster energy transfer to determine the proximity of the dansyl to tryptophans in the peptide. Although we cannot selectively excite any single tryptophan, we can get a picture of the region in which the peptide binds to the protein. With five tryptophans, the maximum apparent efficiency is ~20% if there is only a single active donor in the protein. Since the steady-state and time-resolved measurements both converge on an apparent energy transfer efficiency of >30%, we take this as an indication that multiple donors are involved.This degree of tryptophan quenching corresponds roughly to full quenching of almost two tryptophan residues (which would give ~40% efficiency), something which can only be accomplished if the KE2D15-8 peptide binds to the five-tryptophan side of HCAII. We cannot resolve more than one energy-transfer time constant (140 ps, corresponding to an efficiency of 97%), but it is clear that the dansyl must be quite close to at least two of the tryptophans in the protein.

The usefulness of the energy transfer property of the tryptophan-dansyl pair extends beyond acquiring information about the distance between the peptide and the protein. Given that the efficiency of energy transfer is highly distance-dependent (Eq. 8),

$$E = \frac{R_0^6}{R_0^6 + r^6}, \tag{8}$$

excitation of dansyl via tryptophans in HCAII can in principle also provide information about structural properties. Only the complexes in which the peptide is closely associated with the protein will show sensitized dansyl emission. Thus, by exciting at 290 nm and detecting the dansyl emission, we can selectively probe the complexes with short tryptophan-dansyl distances. Peptides that are more loosely bound, i.e., those in which the dansyl is farther away from the Trp energy donors, cannot efficiently act as acceptors. By comparing the dansyl fluorescence lifetimes obtained through direct excitation with those obtained through energy transfer from Trp, we can confirm our hypothesis that long lifetimes arise from tight complexes only. Indeed, this seems to be to the case: the decaying components of dansyl in the KE2D15-8/HCAII complex when dansyl is excited from tryptophans (290 nm) in HCAII lack the 3.1-ns dansyl fluorescence lifetime that we previously attributed to hydrated, loosely bound structures. The decaying part for indirect excitation only consists of two longer fluorescence lifetimes, centered at ~8 and ~19 ns (Fig. 4 *a*), close to the 8- and 17-ns dansyl fluorescence lifetimes, respectively, obtained by direct excitation. This reinforces the view that the 8-ns and 17/19-ns populations are indeed surface-bound peptides, but with different hydration states and, thus, different well-developed tertiary structures. In the structures where the primary interaction between peptide and protein is through the ligand and linker, rather than directly between peptide and protein, dansyl is hydrated and too far removed from the tryptophans to be excited through energy transfer. Further supporting the notion that indirect excitation probes tight, dehydrated complexes is the fact that the dansyl emission maximum obtained by indirect excitation is shifted to the blue ($\lambda_{max} = 559$ nm; see Fig. 4 *b*) compared to the emission maximum obtained upon direct excitation ($\lambda_{max} = 566$ nm), showing that the indirectly excited dansyls are in a less polar environment than the average dansyl.

CONCLUSIONS

Molecular recognition in peptide/protein systems almost always requires conformational changes in both host and guest. As the interface develops, water is expelled, and contacts form between the two macromolecules. In this article, we show how the transition from the unstructured, loosely bound peptide to the closely bound contact state occurs via structures that differ in their solvation. It is noteworthy, as we show, that these states are in a dynamic equilibrium even when the sensor peptide is fully bound according to equilibrium measurements. The results also have bearing on protein folding: the transitions of the sensor peptide at the protein surface can be seen as a parallel to the sequential formation of secondary and tertiary structure during folding.

The contact surfaces of the uncomplexed forms of the helix-loop-helix scaffold and carbonic anhydrase display disorganized and flexible structures. In the peptide/protein complex, we observe an equilibrium of different binding structures, each with a different degree of tertiary interactions. In the most tightly bound structures, the peptide is rigidly bound to the protein surface, and the interface is fully dehydrated. The second type of structure has a less folded and partly hydrated recognition structure. This structure, we believe, is similar to a molten-globule-like folding intermediate, which constitutes a bimolecular solvent-separated structure that precedes the formation of the fully bound state. In the third type of structure, the peptide scaffold is only weakly associated with the protein surface, and the dansyl probe is almost fully hydrated.

Based on our equilibrium measurements, we conclude that the recognition and binding of the helix-loop-helix scaffold to carbonic anhydrase occurs according to a hierarchical mechanism in which the formation of the dehydrated folded bimolecular state proceeds via a partly hydrated molten-globule-like state. Upon binding and forming the tertiary structure, the peptide scaffold undergoes a disordered-to-ordered transition.

SUPPORTING MATERIAL

Four figures and a table are available at http://www.biophysj.org/biophysj/supplemental/S0006-3495(09)01680-4.

The KE2D15-8 peptide was provided by Professor Lars Baltzer, Uppsala University, whom we also thank for fruitful discussions.

Financial support was given by Ingegerd Berghs stiftelse, Uppsala University, the Carl Trygger Foundation, the Knut and Alice Wallenberg Foundation, and the Swedish Foundation for Strategic Research.

REFERENCES

1. Gavin, A.-C., P. Aloy, …, G. Superti-Furga. 2006. Proteome survey reveals modularity of the yeast cell machinery. *Nature*. 440:631–636.
2. Levy, E. D., and J. B. Pereira-Leal. 2008. Evolution and dynamics of protein interactions and networks. *Curr. Opin. Struct. Biol.* 18:349–357.
3. Zhang, X., C. Schaffitzel, …, S. O. Shan. 2009. Multiple conformational switches in a GTPase complex control co-translational protein targeting. *Proc. Natl. Acad. Sci. USA*. 106:1754–1759.
4. Wang, J., C. Li, …, X. Wang. 2009. Uncovering the rules for protein-protein interactions from yeast genomic data. *Proc. Natl. Acad. Sci. USA*. 106:3752–3757.
5. Pauling, L. 1940. A theory of the structure and process of formation of antibodies. *J. Am. Chem. Soc.* 62:2643–2657.
6. Koshland, D. E. 1958. Application of a theory of enzyme specificity to protein synthesis. *Proc. Natl. Acad. Sci. USA*. 44:98–104.
7. Ma, B., M. Shatsky, …, R. Nussinov. 2002. Multiple diverse ligands binding at a single protein site: a matter of pre-existing populations. *Protein Sci.* 11:184–197.
8. James, L. C., P. Roversi, and D. S. Tawfik. 2003. Antibody multispecificity mediated by conformational diversity. *Science*. 299:1362–1367.
9. Mittag, T., and J. D. Forman-Kay. 2007. Atomic-level characterization of disordered protein ensembles. *Curr. Opin. Struct. Biol.* 17:3–14.
10. Shoemaker, B. A., J. J. Portman, and P. G. Wolynes. 2000. Speeding molecular recognition by using the folding funnel: the fly-casting mechanism. *Proc. Natl. Acad. Sci. USA*. 97:8868–8873.

11. Verkhivker, G. M. 2004. Protein conformational transitions coupled to binding in molecular recognition of unstructured proteins: hierarchy of structural loss from all-atom Monte Carlo simulations of $p27^{Kip1}$ unfolding-unbinding and structural determinants of the binding mechanism. *Biopolymers*. 75:420–433.

12. James, L. C., and D. S. Tawfik. 2005. Structure and kinetics of a transient antibody binding intermediate reveal a kinetic discrimination mechanism in antigen recognition. *Proc. Natl. Acad. Sci. U.S.A.* 102:12730–12735.

13. Sugase, K., H. J. Dyson, and P. E. Wright. 2007. Mechanism of coupled folding and binding of an intrinsically disordered protein. *Nature*. 447:1021–1025.

14. Hulsker, R., M. V. Baranova, …, M. Ubbink. 2008. Dynamics in the transient complex of plastocyanin-cytochrome *f* from *Prochlorothrix hollandica*. *J. Am. Chem. Soc*. 130:1985–1991.

15. Iwahara, J., and G. M. Clore. 2006. Detecting transient intermediates in macromolecular binding by paramagnetic NMR. *Nature*. 440: 1227–1230.

16. Kim, Y. C., C. Tang, …, G. Hummer. 2008. Replica exchange simulations of transient encounter complexes in protein-protein association. *Proc. Natl. Acad. Sci. U.S.A.* 105:12855–12860.

17. Tang, C., J. Iwahara, and G. M. Clore. 2006. Visualization of transient encounter complexes in protein-protein association. *Nature*. 444: 383–386.

18. Renisio, J. G., J. Pérez, …, H. Darbon. 2002. Solution structure and backbone dynamics of an antigen-free heavy chain variable domain (VHH) from Llama. *Proteins*. 47:546–555.

19. Namanja, A. T., T. Peng, …, J. W. Peng. 2007. Substrate recognition reduces side-chain flexibility for conserved hydrophobic residues in human Pin1. *Structure*. 15:313–327.

20. Dill, K. A., S. B. Ozkan, …, T. R. Weikl. 2008. The protein folding problem. *Annu. Rev. Biophys*. 37:289–316.

21. Dill, K. A., and H. S. Chan. 1997. From Levinthal to pathways to funnels. *Nat. Struct. Mol. Biol*. 4:10–19.

22. Levy, Y., S. S. Cho, …, P. G. Wolynes. 2005. A survey of flexible protein binding mechanisms and their transition states using native topology based energy landscapes. *J. Mol. Biol*. 346:1121–1145.

23. Levy, Y., and J. N. Onuchic. 2006. Water mediation in protein folding and molecular recognition. *Annu. Rev. Biophys. Biomol. Struct*. 35: 389–415.

24. Petrone, P. M., and A. E. Garcia. 2004. MHC-peptide binding is assisted by bound water molecules. *J. Mol. Biol*. 338:419–435.

25. Oliveberg, M., and P. G. Wolynes. 2005. The experimental survey of protein-folding energy landscapes. *Q. Rev. Biophys*. 38:245–288.

26. Andersson, T., M. Lundquist, …, L. Baltzer. 2005. The binding of human carbonic anhydrase II by functionalized folded polypeptide receptors. *Chem. Biol*. 12:1245–1252.

27. Enander, K., G. T. Dolphin, and L. Baltzer. 2004. Designed, functionalized helix-loop-helix motifs that bind human carbonic anhydrase II: a new class of synthetic receptor molecules. *J. Am. Chem. Soc*. 126:4464–4465.

28. Habenicht, A., J. Hjelm, …, L. B. A. Johansson. 2002. Two-photon excitation and time-resolved fluorescence: 1. The proper response function for analysing single-photon counting experiments. *Chem. Phys. Lett*. 354:367–375.

29. Vinogradov, S. A., and D. F. Wilson. 2000. Recursive maximum entropy algorithm and its application to the luminescence lifetime distribution recovery. *Appl. Spectrosc*. 54:849–855.

30. Lignell, M., L. Tegler, and H.-C. Becker. 2009. Hydrated and dehydrated tertiary interactions—opening and closing—of a four-helix bundle. *Biophys. J*. 97:572–580.

31. Olofsson, S., and L. Baltzer. 1996. Structure and dynamics of a designed helix-loop-helix dimer in dilute aqueous trifluoroethanol solution. A strategy for NMR spectroscopic structure determination of molten globules in the rational design of native-like proteins. *Fold. Des*. 1:347–356.

32. Olofsson, S., G. Johansson, and L. Baltzer. 1995. Design, synthesis and solution structure of a helix-loop-helix dimer: a template for the rational design of catalytically active polypeptides. *J. Chem. Soc. Perkin Trans*. 2:2047–2056.

33. Baltzer, L. 2007. Polypeptide conjugate binders for protein recognition. *In* Creative Chemical Sensor Systems. T. Schrader, editor. Springer, Berlin. 89–106.

34. Lakowicz, J. R. 1999. The Perrin Equation—rotational motion of proteins. *In* Principles of Fluorescence Spectroscopy. Kluwer Academic/Plenum Publishers, New York 304–305.

35. Kulinski, T., A. B. A. Wennerberg, …, T. Bartfai. 1997. Conformational analysis of galanin using end to end distance distribution observed by Förster resonance energy transfer. *Eur. Biophys. J*. 26:145–154.

36. Gilson, M. K., and B. H. Honig. 1986. The dielectric constant of a folded protein. *Biopolymers*. 25:2097–2119.

37. Simonson, T., and D. Perahia. 1995. Internal and interfacial dielectric properties of cytochrome *c* from molecular dynamics in aqueous solution. *Proc. Natl. Acad. Sci. U.S.A.* 92:1082–1086.

38. Raghuraman, H., and A. Chattopadhyay. 2003. Organization and dynamics of melittin in environments of graded hydration: a fluorescence approach. *Langmuir*. 19:10332–10341.

39. Haldar, S., H. Raghuraman, and A. Chattopadhyay. 2008. Monitoring orientation and dynamics of membrane-bound melittin utilizing dansyl fluorescence. *J. Phys. Chem. B*. 112:14075–14082.

40. Arai, M., K. Kuwajima, and C. R. Matthews. 2000. Role of the molten globule state in protein folding. *Adv. Protein Chem*. 53:209–282.

41. Ptitsyn, O. B. 1995. Molten globule and protein folding. *Adv. Protein Chem*. 47:83–229.

42. Cheung, M. S., A. E. García, and J. N. Onuchic. 2002. Protein folding mediated by solvation: water expulsion and formation of the hydrophobic core occur after the structural collapse. *Proc. Natl. Acad. Sci. USA*. 99:685–690.

43. Sessions, R. B., G. L. Thomas, and M. J. Parker. 2004. Water as a conformational editor in protein folding. *J. Mol. Biol*. 343:1125–1133.

44. Håkansson, K., M. Carlsson, …, A. Liljas. 1992. Structure of native and apo carbonic anhydrase II and structure of some of its anion-ligand complexes. *J. Mol. Biol*. 227:1192–1204.